NANO LETTERS

2009
Vol. 9, No. 5
2021-2025

Smart Tissue Culture: in Situ Monitoring of the Activity of Protease Enzymes Secreted from Live Cells Using Nanostructured Photonic Crystals

Kristopher A. Kilian,[†] Leo M. H. Lai,[†] Astrid Magenau,[‡] Siân Cartland,[‡] Till Böcking,[†,§] Nick Di Girolamo,[||] Michael Gal,[§] Katharina Gaus,[‡] and J. Justin Gooding*[,†]

School of Chemistry, Centre for Vascular Research, Department of Pathology, and School of Physics, University of New South Wales, Sydney, New South Wales 2052, Australia

Received January 27, 2009; Revised Manuscript Received April 6, 2009

ABSTRACT

Monitoring enzyme secretion in tissue culture has proved challenging because to date the activity cannot be continuously measured in situ. In this Letter, we present a solution using biopolymer loaded photonic crystals of anodized silicon. Shifts in the optical response by proteolytic degradation of the biopolymer provide label-free sensing with unprecedented low detection limits (1 pg) and calculation of kinetic parameters. The enhancement in sensitivity relative to previous photonic crystal sensors constitutes a change in the sensing paradigm because here the entire pore space is responsive to the secreted enzyme rather than just the pore walls. In situ monitoring is demonstrated by detecting secretion of matrix metalloprotease 9 from stimulated human macrophages.

Monitoring secreted biomolecules during cell-based assays is important for fundamental research, bioengineering, toxicology, and drug discovery.[1−3] For example, extracellular proteolytic enzymes are critical players in tissue remodeling, cell migration, and the immune response to infection and disease.[4,5] Toward the goal of an in situ assay for monitoring cells in culture, most attention has been devoted to the design of devices that report on the cellular environment, such as electrical sensing (impedance),[6] intra- and extracellular potential,[7−9] and interferometric approaches.[10,11] However, despite the power of these techniques, they provide no information about the activity of effector molecules released by the cells. Nanoporous silicon (PSi) is a promising material for live cell assays primarily due to its biocompatibility,[12] tunable nanoarchitecture, and versatility for optical biosensing.[13−15] Sailor and colleagues first reported the use of PSi as a cell culture substrate for noninvasively monitoring of changes in cell morphology by light scattering at the interface.[10,11] In addition, others have shown that PSi can be used as a biomaterial sensitive to extracellular signals via changes in the optoelectronic and photoluminescence properties of the material.[16−18] Despite these advances, none of these examples has provided a system for detecting specific biomolecules secreted from living cells.

In conventional photonic crystal biosensing, optical signals arise from the adsorption to or loss of material from the pores causing a change in the average refractive index in the structure. However, these changes only occur at the pore walls and hence the refractive index of the majority of the pore volume remains unchanged. Hence optical signals will be expected to be greatly enhanced if the refractive index of the entire pore volume was changed. Here we incorporate protease-responsive biopolymers that fill the entire pore space of the photonic crystal. The enzymatic removal of the biopolymer from the pores yields a blue shift in the photonic crystal reflectivity and therefore provides a label-free method of detecting protease activity.

We chose as the optical sensor a PSi-based rugate filter[19−21] that displays a narrow, resonant reflectance peak whose position is sensitive to the infiltrating biological species. The mean pore size of our PSi device was 50 nm. Surface modification of the PSi is required to protect the PSi from oxidation in aqueous environments, reduce nonspecific adsorption of biomolecules, and covalently attach the gelatin polypeptides. The surface modification was achieved using a multistep covalent coupling methodology involving hydrosilylation of 10-succinimidyl undecenoate (1), coupling of the antifouling EG_6 species (2), activation using disuc-

* Corresponding author, justin.gooding@unsw.edu.au.
[†] School of Chemistry.
[‡] Centre for Vascular Research.
[§] School of Physics.
[||] Department of Pathology.

10.1021/nl900283j CCC: $40.75
Published on Web 04/21/2009

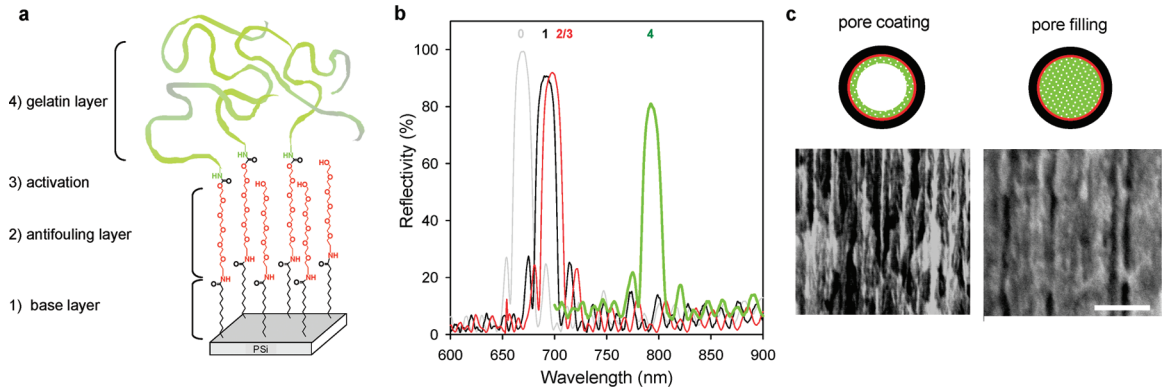

Figure 1. (a) Schematic representation of chemical layers grafted within mesoporous PSi: (1) base layer formed by hydrosilylation of 10-succinimidyl undecenoate onto the Si−H surface (black), (2) coupling of hexa(ethylene glycol) amine (red), (3) activation with DSC, and (4) immobilization of gelatin (green). (b) Optical crystal reflectivity red shifts for organic derivatization from (a), surfaces 0 → 1 (22 nm), 1 → 2/3 (6 nm), and 3 → 4 (94 nm). (c) Illustration of the nanostructured pores with the pore walls coated with biopolymer (refractive index, n_{gel} (∼1.4) + n_{air} (∼1.0)) and when the entire volume is filled (refractive index, n_{gel} (∼1.4)) yielding a larger average refractive index (biopolymer in green). Scanning electron micrographs showing a side view of the PSi nanostructure without (left) and with (right) gelatin immobilization. Scale bar = 200 nm.

cinimidyl carbonate (DSC) (3), and gelatin immobilization (4) (Figure 1a). Each chemical step resulted in a change in average refractive index of the PSi photonic crystal and was monitored by reflectivity spectroscopy to evaluate the changes in the position of the stop band (Figure 1b). Throughout each derivatization step the full width at half-maximum of the high reflectivity peak remained relatively unchanged at 15−18 nm indicating that the surfaces have been homogeneously modified throughout the entire structure. The larger shift with gelatin is caused by the polypeptide filling the entire pore volume compared with earlier work where only the pore walls were modified[14] (Figure 1c). Importantly, the difference between the reflectivity shift of the structure containing water and the structure containing a gelatin hydrogel is on the order of 10−40 nm. Therefore, gelatin cleavage by protease enzymes should be easily detected in real time by monitoring blue shifts in the optical reflectivity (see Supporting Information for optimization and spectroscopic analysis of each chemical step, Supplementary Figures 1, 2, and 3).

PSi rugate filters containing gelatin hydrogels were initially exposed to the protease subtilisin to define the detection limit compared to our previous work.[14] Digestion of gelatin by subtilisin was monitored by measuring the blue shift in the reflectivity as organic material (n = ∼1.4) is replaced with water (n = 1.33) in the pores (Figure 2a,b). A high concentration of subtilisin (9.15 μM) in solution shifted the reflectivity peak position by 15 nm (approximately 70% gelatin digestion) in 15 min (Figure 2b). Monitoring the PSi over a range of concentrations, we found a limit of detection of 0.37 pM (1 pg of subtilisin in 100 μL) detected within 30 min (Figure 2c). Significantly, detecting subtilisin activity by exploiting the larger refractive index change as a consequence of altering the entire pore space allows a greater than 1000-fold increase in sensitivity compared to previously reported label-free optical protease sensors.[14,15,22,23] This improvement makes PSi rugate filters as sensitive as fluorometric immunoassays and electrophoretic techniques (zymography)[2] without any labeling requirements or sophisticated read-out instrumentation.

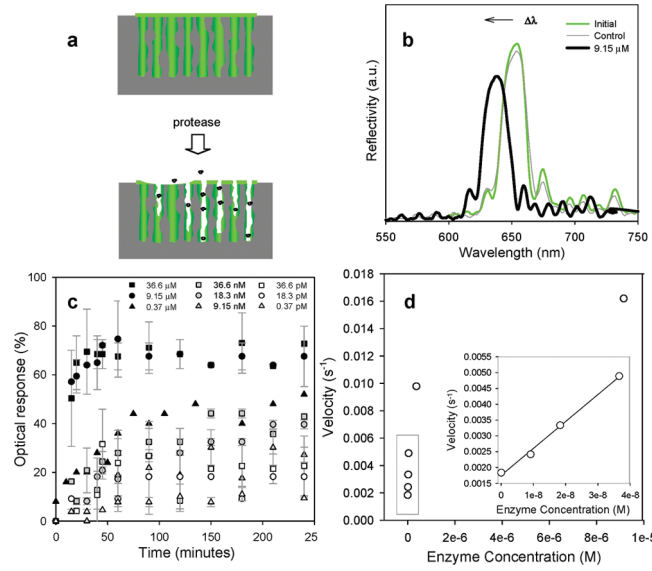

Figure 2. (a) Schematic depiction of gelatin-loaded pores before and after proteolysis. (b) Change in the position of the filter stop band after exposure to protease when gelatin-filled PSi was exposed to 9.15 μM subtilisin demonstrating a pronounced blue shift (black). (c) Real-time optical response of gelatin-loaded rugate filters exposed to subtilisin in solution from picomoles per liter to micromoles per liter. The optical response (%) is calculated as $(\Delta\lambda_{protease} - \Delta\lambda_{control}/\Delta\lambda_{gelatin}) \times 100$, where $\Delta\lambda_{protease}$ is the blue shift of the filter resonance after exposure to protease, $\Delta\lambda_{control}$ is the shift of the control sample (no enzyme), and $\Delta\lambda_{gelatin}$ is the initial red shift upon gelatin immobilization. Error bars represent standard deviations of two to four replicate experiments performed with different PSi surfaces on different days. (d) Calculated proteolytic velocity for protease concentrations from (c). Inset: linear correlation observed from picomoles per liter to nanomoles per liter (R^2 = 0.996).

Because of the large internal surface area and pore volume, Michaelis−Menten kinetics applies at low enzyme concentrations (less than micromoles per liter). Hence, the slope of the curves for gelatin digestion (Figure 2c) can be modeled

Table 1. Calculated Number of Subtilisin Molecule per Pore and Corresponding Velocities for Different Concentrations[a]

[subtilisin] (M)	no. of molecules/pore	velocity (s^{-1})
3.66×10^{-5}	60000	—
9.15×10^{-6}	15000	0.016
7.00×10^{-7}	1000	0.0097
3.66×10^{-8}	**60**	**0.0049**
1.83×10^{-8}	**30**	**0.0033**
9.15×10^{-9}	**15**	**0.0024**
1.83×10^{-11}	**0.03**	**0.0018**
3.66×10^{-13}	0.0006	—
3.66×10^{-14}	0.00006	—

[a] Bold type indicates operating regime where kinetic assumptions hold. Dash line indicates no measurable slope at very high and very low concentrations.

to obtain velocity (initial rate of substrate proteolysis) assuming that mass transport is not limiting and the interfacial substrate concentration is in excess of the amount of enzyme. For the former, this is a reasonable assumption for a thin film of enzyme solution above the PSi (<5 mm thick). For the latter, enzyme concentrations <0.37 μM satisfy the criteria that the substrate is in excess of enzyme; i.e., the number of enzymes per pore is small and thus there is no competition for substrate binding (see Table 1). By plotting proteolytic velocity as a function of input subtilisin concentration (Figure 2d), it is evident that the velocity increases with enzyme concentration before plateauing in the micromoles per liter range as the subtilisin concentration approaches and exceeds the immobilized gelatin concentration (>1000 subtilisin molecules per pore) at which point the assumptions no longer apply. Proteolytic velocity at enzyme concentrations below micromoles per liter yields a linear relationship to enzyme concentration (Figure 2d, inset). Using a concentration of substrate in the nanoporous scaffold of ~15 mM (the concentration of gelatin applied to the PSi), k_{cat}/K_m is equal to $\sim 2.3 \times 10^6$ M^{-1} s^{-1} (see Supporting Information for derivation). To compare the activity of subtilisin for gelatin without the nanoporous scaffold, a solution phase assay was performed that emulates an idealized scenario for proteolysis.

The solution phase assay yielded a very similar k_{cat}/K_m of $\sim 2.6 \times 10^6$ M^{-1} s^{-1} (see Supplementary Figure 4 in Supporting Information). This indicates that the presence of the nanoporous scaffold is not impeding the enzyme from digesting the gelatin.

To demonstrate the utility of the PSi sensor for in situ monitoring of cellular activity, we next demonstrated the ability to detect the enzymatic activity of matrix metalloproteinases (MMPs). Human monocyte-derived macrophages (HMDMs) are known to secrete the gelatinolytic MMP-9 under physiological and pathological conditions to model and remodel the extracellular matrix (ECM). In situ detection of MMPs is therefore of interest in wound healing, cell migration, and tissue morphogenesis as overproduction and deregulation of MMPs secretion contributes to inflammation, cardiovascular disease, and cancer.[24−26] MMP-2 (pro 72 kDa, active 62 kDa) and MMP-9 (pro 92 kDa, active 84 kDa) are

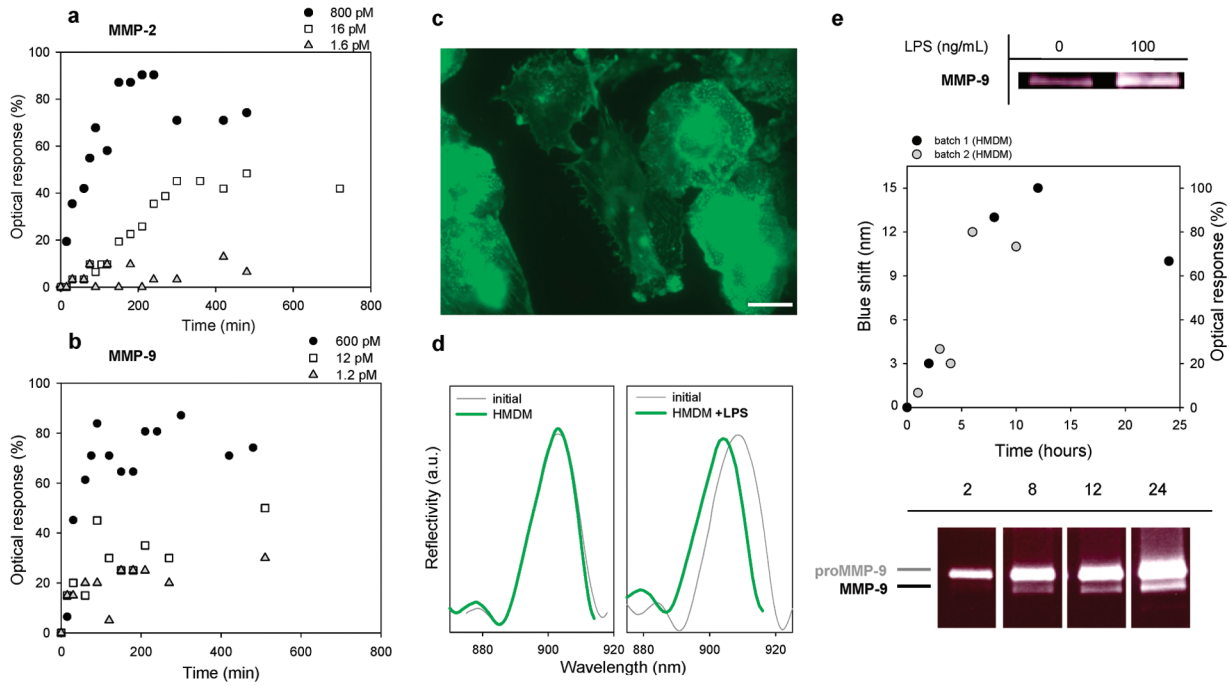

Figure 3. (a, b) Optical response of gelatin-loaded PSi rugate filters normalized to control (no enzyme) at three concentrations of recombinant active MMP-2 and MMP-9, respectively. (c) Phalloidin staining of F-Actin in HMDMs shows cells adhered to the gelatin-loaded surface after LPS stimulation for 24 h. Scale bar is 20 μm. (d) reflectivity spectra showing the raw optical response to unstimulated (left) and LPS stimulated HMDMs after 24 h (right). (e) Top: zymogram of supernatants from HMDMs treated with or without 100 ng/mL LPS for 12 h. Middle: blue shift in the photonic resonance $[(\Delta\lambda_{HMDM+LPS} - \Delta\lambda_{media+LPS}) - (\Delta\lambda_{HMDM} - \Delta\lambda_{media})]$ and corresponding optical response (eq 1) of rugate filters exposed to different batches of macrophages stimulated with LPS over time. Bottom: Gelatin zymograms of supernatants from the same PSi surfaces as batch 1 above after optical measurement showing increasing levels of MMP-9 secretion over time (upper band, proform; lower band, active form).

significantly larger than subtilisin (27 kDa), and therefore it was important to determine if these MMPs could enter the pores of the photonic crystal and hydrolyze the immobilized gelatin. Active recombinant MMP-2 and MMP-9 were assayed over a range of concentrations. Monitoring the exposure of the optical crystals in real time to different concentrations of MMPs yield optical response curves that demonstrate infiltration of enzyme. Gelatin proteolysis was detected down to 1−2 pM (approximately 1 ng in 100 μL) for MMP-9 within 1 h (Figure 3b).

To stimulate the release of MMP-9 from live cells, macrophages were stimulated with lipopolysaccharide (LPS). LPS is a surface component of Gram-negative bacteria, recognized by macrophages to initiate an immune response. LPS treatment of macrophages has been shown to cause upregulation of MMP-9.[27,28] HMDMs were seeded on gelatin-loaded optical crystals in a 24-well plate, allowed to adhere for 2 h, followed by LPS stimulation (100 ng/mL). To account for signal drift when exposed to physiological conditions, surfaces were divided into four pieces, incubated with "HMDMs", "HMDMs+LPS", "media", and "media+LPS", respectively, with optical response defined as

$$\text{optical response } (\%) = \left[\frac{(\Delta\lambda_{\text{HMDM+LPS}} - \Delta\lambda_{\text{media+LPS}}) - (\Delta\lambda_{\text{HMDM}} - \Delta\lambda_{\text{media}})}{\Delta\lambda_{\text{gelatin}}}\right] \times 100 \quad (1)$$

where the quantity $[(\Delta\lambda_{\text{HMDM+LPS}} - \Delta\lambda_{\text{media+LPS}}) - (\Delta\lambda_{\text{HMDM}} - \Delta\lambda_{\text{media}})]$ is the normalized blue shift in the optical spectra and $\Delta\lambda_{\text{gelatin}}$ is the initial gelatin red shift (see Supplementary Figure 5 in Supporting Information for schematic). HMDMs remained adherent and viable on the PSi surface after incubation overnight as determined by F-Actin immunofluorescence (Figure 3c). Exposure to HMDMs in culture for 24 h led to no significant shift in the reflectivity maximum (Figure 3d, left). However, when rugate filters were exposed to HMDMs treated with LPS in the same experiment, a pronounced blue shift in the spectrum was evident (Figure 3d, right). Secretion of MMPs induced by LPS treatment is also detected by gelatin zymography (Figure 3e, top). The PSi sensor responded to secreted MMPs after 1 h, and the optical response increased with incubation time for the first 12 h as expected with continuous secretion during LPS stimulation (Figure 3e, middle). The decrease in optical response after 24 h is presumably on account of physisorbed material within the nanopores inducing a red shift thus counteracting the proteolytic blue shift in the photonic resonance as observed previously at high concentrations of enzyme.[14] For verification of MMP activity, supernatants from the plate were removed at the indicated time points and displayed on gelatin zymography gels (Figure 3e, bottom). Active MMP-9 generated from the adherent macrophages is detected by zymography after 2 h of LPS stimulation which supports the PSi optical results.

In summary, we present a strategy for enhancing the sensitivity of photonic crystals such that the release of proteases from live cells can be monitored in real time. The conceptual advance that makes this possible is to ensure that the average refractive index of the photonic crystal, and hence the optical signature, is influenced by the entire pore spaces of the crystal rather than just the pore walls. For monitoring protease activity this is achieved by incorporating soft polypeptide biopolymers within the hard nanostructure of photonic crystals. Cleavages of the polypeptides by proteases cause the required change in refractive index and hence shift in optical signal. Chemical modification of the underlying silicon prior to gelatin immobilization increases the stability of the material, allowing storage of the photonic crystals for 4 months under ambient conditions with very little signal drift (Supplementary Figure 6 in Supporting Information). These composite structures are easily fabricated by established methods, the dissolution product is nontoxic, and the methodology is applicable for a wide array of biopolymers. For instance casein, fibrin, and similar macromolecules specific to certain types of MMPs could tune the response of the sensor. Alternatively, biological and biomimetic copolymer systems[29] could be readily incorporated with this system for highly specific real-time optical biosensing. The area of spectral collection can be reduced down to micrometers, potentially allowing monitoring of response of single cells. Incorporating photonic crystals into tissue culture plates and using simple light sources will allow routine integration of these components with cell-based assays.

Acknowledgment. This research was supported by the Australian Research Council's Discovery Projects funding scheme (project number DP0772356).

Supporting Information Available: Details of materials and methods, reflectivity spectroscopy, Fourier transform infrared (FTIR) spectroscopy, solution phase protease assays, and shelf life data. This material is available free of charge via the Internet at http://pubs.acs.org.

References

(1) Girard, C.; Michaud, D. *Anal. Biochem.* **2002**, *308*, 388.
(2) Lombard, C.; Saulnier, J.; Wallach, J. *Biochimie* **2005**, *87*, 265.
(3) Fang, Y. *Assay Drug Dev. Technol.* **2006**, *4*, 583.
(4) Garcia-Touchard, A.; Henry, T. D.; Sangiorgi, G.; et al. *Arterioscler., Thromb., Vasc. Biol.* **2005**, *25*, 1119.
(5) Singh, R. B.; Dandekar, S. P.; Elimban, V.; et al. *Mol. Cell. Biochem.* **2004**, *263*, 241.
(6) Spegel, C.; Heiskanen, A.; Daehli Skjolding, L. H.; et al. *Electroanalysis* **2008**, *20*, 680.
(7) Hug, T. S. *Assay Drug Dev. Technol.* **2003**, *1*, 479.
(8) Kovacs, G. T. A. *Proc. IEEE* **2003**, *91*, 915.
(9) Pancrazio, J. J.; Whelan, J. P.; Borkholder, D. A.; et al. *Ann. Biomed. Eng.* **1999**, *27*, 697.
(10) Schwartz, M. P.; Derfus, A. M.; Alvarez, S. D.; et al. *Langmuir* **2006**, *22*, 7084.
(11) Alvarez, S. D.; Schwartz, M. P.; Migliori, B.; et al. *Phys. Status Solidi A* **2007**, *204*, 1439.
(12) Chin, V.; Collins, B. E.; Sailor, M. J.; et al. *Adv. Mater.* **2001**, *13*, 1877.
(13) Bonanno, L. M.; DeLouise, L. A. *Langmuir* **2007**, *23*, 5817.
(14) Kilian, K. A.; Böcking, T.; Gaus, K.; et al. *ACS Nano* **2007**, *1*, 355.
(15) Orosco, M. M.; Pacholski, C.; Miskelly, G. M.; et al. *Adv. Mater.* **2006**, *18*, 1393.
(16) Bayliss, S. C.; Buckberry, L. D.; Fletcher, I.; et al. *Sens. Actuators, A* **1999**, *A74*, 139.
(17) Ben-Tabou de-Leon, S.; Oren, R.; Spira, M. E.; et al. *Phys. Status Solidi A* **2005**, *202*, 1456.
(18) Kilian, K. A.; Böcking, T.; Gaus, K.; et al. *Angew. Chem., Int. Ed.* **2008**, *47*, 2697.
(19) Ilyas, S.; Böcking, T.; Kilian, K.; et al. *Opt. Mater.* **2007**, *29*, 619.

(20) Böcking, T.; Kilian, K. A.; Gaus, K.; et al. *Adv. Funct. Mater.* **2008**, *18*, 3735.
(21) Kilian, K. A.; Böcking, T.; Gaus, K.; et al. *Biomaterials* **2007**, *28*, 3055.
(22) Millington, R. B.; Mayes, A. G.; Blyth, J.; et al. *Anal. Chem.* **1995**, *67*, 4229.
(23) Millington, Roger B.; Mayes, Andrew G.; Blyth, Jeff; et al. *Sens. Actuators, B* **1996**, *B33*, 55.
(24) Stamenkovic, I. *J.Pathology* **2003**, *200* (4), 448.
(25) Konttinen, T. T.; Ainola, M.; Valleala, H.; et al. *Ann. Rheum. Dis.* **1999**, *58*, 691.
(26) Coussens, L. M.; Fingleton, B.; Matrisian, L. M. *Science* **2002**, *295*, 2387.
(27) Xie, B.; Dong, Z.; Fidler, I. J. *J. Immunol.* **1994**, *152*, 3637.
(28) Bergin, P. J.; Sicheng, W.; Qiang, P.-H.; et al. *FEMS Immunol. Med. Microbiol.* **2005**, *45*, 159.
(29) Lutolf, M. P.; Hubbell, J. A. *Nat. Biotechnol.* **2005**, *23*, 47.

NL900283J